frontiers | Frontiers in Marine Science

TYPE Original Research
PUBLISHED 17 July 2023
DOI 10.3389/fmars.2023.1222810

OPEN ACCESS

EDITED BY
Jose Luis Iriarte,
Austral University of Chile, Chile

REVIEWED BY
Ichiro Imai,
Hokkaido University, Japan
Jane Theophline Bhaskar,
National Centre for Polar and Ocean Research (NCPOR), India

*CORRESPONDENCE
Shizuka Ohara
oharashizu@hiroshima-u.ac.jp

RECEIVED 16 May 2023
ACCEPTED 26 June 2023
PUBLISHED 17 July 2023

CITATION
Ohara S, Yano R, Furuya K, Sato T, Ikeda S and Koike K (2023) The effects of sea-bottom plowing on phytoplankton assemblages: a case study of northern Hiroshima Bay, the Seto Inland Sea of Japan. *Front. Mar. Sci.* 10:1222810. doi: 10.3389/fmars.2023.1222810

The effects of sea-bottom plowing on phytoplankton assemblages: a case study of northern Hiroshima Bay, the Seto Inland Sea of Japan

Shizuka Ohara[1]*, Ryoko Yano[1], Kenichiro Furuya[2], Takafumi Sato[2], Syunichiro Ikeda[3] and Kazuhiko Koike[1]

[1]Graduate School of Integrated Sciences for Life, Hiroshima University, Higashihiroshima, Japan, [2]Fisheries Division, Agriculture, Forestry, and Fisheries Department, Economic Affairs and Tourism Bureau, Hiroshima, Hiroshima, Japan, [3]Hiroshima City Agriculture, Forestry and Fisheries Promotion Center, Hiroshima, Japan

Sea-bottom plowing is originally a method used to oxidize sediment by stirring the bottom with a trawl fishing tool, and its effect in increasing primary productivity of the water column was investigated in the western part of the Seto Inland Sea of Japan. Preliminary field sampling showed that diatom resting stage cells were abundant in the sediment of the tested area at 1.5–2.6 × 10^5 MPN g^{-1} wet sediment. When the sediment was added to filtered seawater, diatom cells emerged from the sediment after one day and increased more drastically under a light level corresponding to sunny weather than cloudy weather. In the actual trials of sea-bottom plowing on the field for a continuous period of 4 years, dissolved inorganic nutrients increased at the bottom layer after the plowing and promoted photosynthetic activities of the phytoplankton communities in 2018 and 2021. Chlorophyll *a* concentration at the middle layers increased 1.06–2.15 times after plowing throughout the trials for 4 years. Diatoms contributed to 67–99% of this chlorophyll *a* concentrations and included the genera *Skeletonema* and *Chaetoceros*, which formed resting-stage cells in the sediment. *Pseudo-nitzschia* spp. often increased after the plowing, which was assumed to be of seawater origin. Estimated primary productivities of the middle layers dropped once the following day due to turbid water caused by the plowing but increased 2.03–4.41 times after two or five days in 2018, 2019, and 2021. These results suggest that sea-bottom plowing has an enrichment effect on diatoms and could be a possible measure to fertilize the sea.

KEYWORDS

diatoms, flagellates, nutrients, productivity, resting-stage-cells, cysts, sea-bottom-plowing

1 Introduction

The Seto Inland Sea (Figure 1A), the largest semi-enclosed sea area of Japan, had once experienced severe red tides due to eutrophication. To mitigate eutrophication, the Interim Law for Conservation of the Environment of the Seto Inland Sea (hereafter called "the Setouchi Law") was enacted in 1973, and the total nitrogen and phosphorus concentrations in wastewater discharged into the sea have been reduced stepwise, which has resulted in decreases in dissolved inorganic nitrogen (DIN) and phosphorus (DIP) (Abo and Yamamoto, 2019). This action has largely contributed to lowering the incidences of red tide and fishery damage (Setonaikai Fisheries Coordination Office, 2021a), but in return, this sea is now undergoing oligotrophication. Total fish catch has decreased to one-third from the peak in the 1980s (Setonaikai Fisheries Coordination Office, 2021b) which is presumably caused by a decline in biological productivity along with oligotrophication (Abo and Yamamoto, 2019). The Setouchi Law was recently revised to include an article that requires appropriate management of DIN and DIP to increase fish production (Ministry of the Environment, 2018). However, as eutrophication elements, further loading of DIN and DIP to the area is still under debate and lacks societal consensus, and this issue will probably require long-term discussion. Meanwhile, other strategies are needed to address the decreased fishing activity.

Sea-bottom plowing is an attempt to improve fishing grounds by oxidizing sediment by stirring the bottom with simple trawling gear. Recently, this method has been widely practiced in various

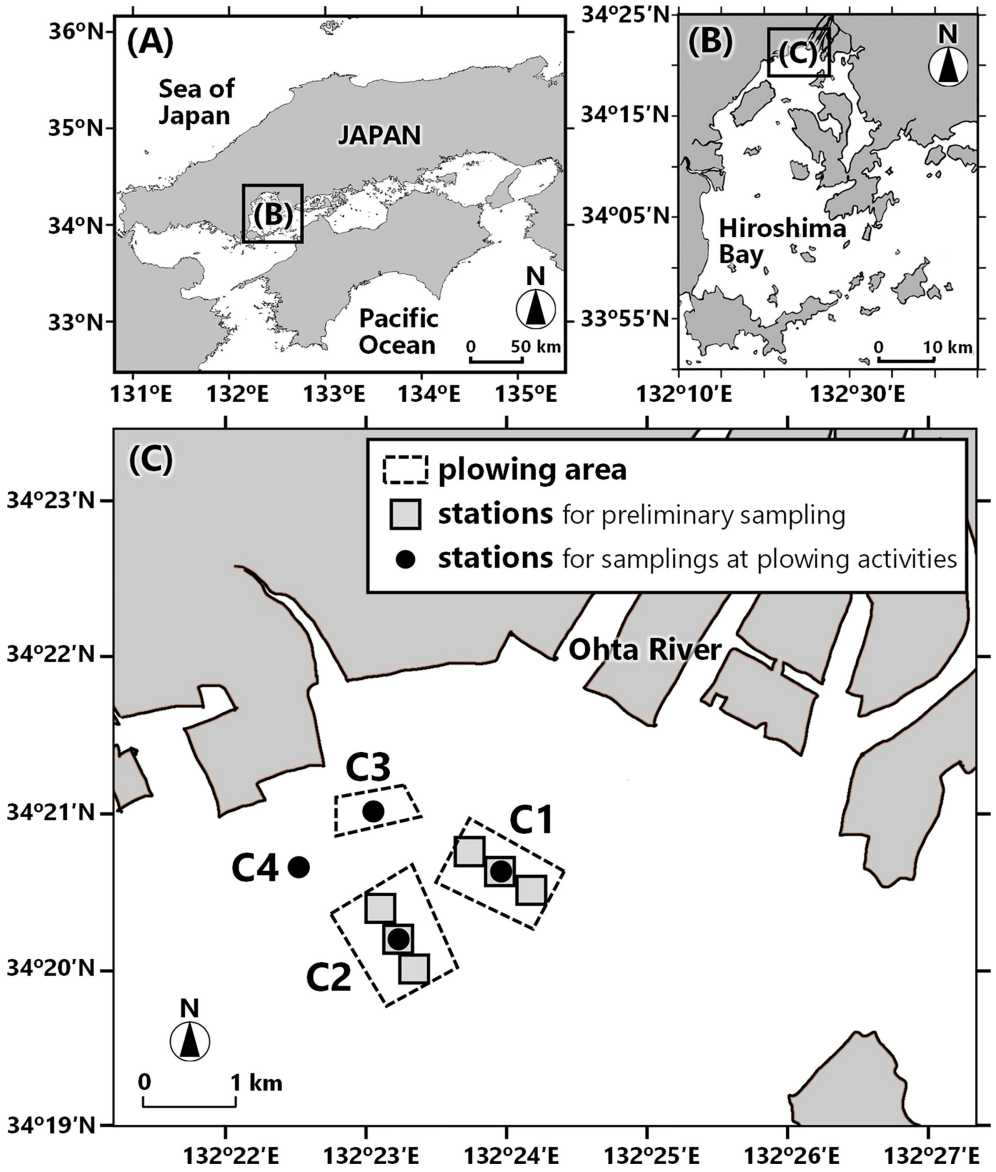

FIGURE 1
Maps of the Seto Inland Sea, Japan **(A)**, Hiroshima Bay **(B)**, plowing areas and sampling stations in northern Hiroshima Bay **(C)**. Dotted squares indicate the plowing areas. Stations for the preliminary sampling are shown by gray boxes in areas C1 and C2. Black points indicate the stations for field monitoring at actual plowing activities (see text for details).

places along the coast of Japan (Nakanishi et al., 2012; Imai et al., 2017; Ministry of the Environment, 2018). In addition to its effectiveness in improving the bottom environment, sea-bottom plowing is expected to supply inorganic nutrients to the water columns and increase phytoplankton growth resulting in increased primary productivity. DIN and DIP-rich sediment pore water can be diffused into the water *via* sea-bottom plowing (Nakanishi et al., 2012; Imai et al., 2017; Ministry of the Environment, 2018). Similar but natural events leading to chl. *a* and primary production increases were reported after cyclones and typhoons (Zeeman, 1985; Tsuchiya et al., 2013; Kuttippurath et al., 2021). In those cases, diatoms, the main primary producers of the coastal food chain, often increased. They form resting stage cells due to environmental stresses, such as nutrient deficiency, (Hargraves and French, 1983; Garrison, 1984; Itakura, 2000) and germinate immediately upon the improvement of the environment and use light as a trigger (Hollibaugh et al., 1981; Hargraves and French, 1983; Koizumi et al., 1997). Diatom increase by sea-bottom plowing possibly caused by the dispersal of the diatoms' resting cells to the photic layer was also reported (Imai et al., 2017) but has not yet been scientifically evidenced. In this study, we aimed to clarify whether sea-bottom plowing could actually contribute to increased primary production of the water column by promoting the germination of diatom resting stage cells and by supplying nutrient-rich bottom water. The study area, Hiroshima Bay, located in the western part of the Seto Inland Sea (Figures 1A, B), is the second highest primary productive area in the Seto Inland Sea after Osaka Bay (Tada et al., 1998), and therefore, it is a highly oligotrophic area. This bay is an important area for aquaculture industries, especially for the Pacific oyster (*Crassostrea gigas*) with a production accounting for 61.3% of the total production in Japan (Ministry of Agriculture, Forestry and Fisheries, 2021). Meanwhile, the industry has been facing notable decreases in the production and insufficient supply of natural oyster larvae (Hiroshima City Fisheries Promotion Center, 2021). This issue is argued to be as a result of decreases in phytoplankton including diatoms. Therefore, we cooperated with the local fishermen union and conducted sea-bottom plowings at Hiroshima Bay mainly in June from 2018 until 2021, aiming to contribute to the improvement of the fishing ground for the oyster culture and to gain scientific evidence for its potential to lead to increased phytoplankton growth and primary production.

2 Materials and methods

2.1 Study site

Figures 1B, C show the plowing sites of northern Hiroshima Bay. The area faces the river mouth of Ohta River and is the largest fishing ground for the oyster culture. The bottom depths of the sampling stations were 11.8–15.0 m (mean 13.4 m).

2.2 Preliminary field sampling and experiments

2.2.1 The estimation of densities of diatom resting stage cells in sediments

Prior to sea-bottom plowing activities, an abundance of diatoms' resting stage cells and cysts of harmful flagellates in the bottom sediments were investigated except in 2020. Sediment collections using an Ekman-Birge grab sampler were done at three points of the scheduled plowing area; area C1 (Figure 1C) in February 2018 and area C2 in May 2019 and May 2021. Subsurface sediments down to 2 cm depth from the surface were transported to the laboratory and stored at 10°C in the dark. The sediments from the three stations were mixed evenly and used to determine the number of resting stage cells of phytoplankton by employing a methodology of the most probable number (MPN) by Imai et al. (1990). The photosynthetic photon flux density (PPFD) was set to 70 µmol-photons m^{-2} sec^{-1} (L:D=14:10 h), and a modified SWM-III medium was used (Imai, 2012). The incubator was set at 21°C in accordance with the field environment of Hiroshima Bay in June when the plowing was carried out. To determine phytoplankton germination other than diatoms, a medium with 1 mg L^{-1} germanium dioxide (GeO_2) was used to suppress the growth of diatoms. After 7–9 days of incubation under the above conditions, germinated cells were identified under a fluorescence microscope (IX 71, Olympus, Tokyo, Japan) to calculate the number of resting-stage cells or cysts.

2.2.2 Laboratory culture experiments simulating the germination of phytoplankton resting stages

Prior to the first plowing activity in 2018, culture experiments were performed to know the potential of germination in phytoplankton species, which could be done by partly simulating possible phytoplankton increase after sea-bottom plowing. The same sediment sample used in the above MPN experiment in 2018, one gram of the mixed sediment, was added to 5 L of sterilized filtered seawater collected at the same site (3 m depth) with additions of NO_3-N, 37.5 µM; PO_4-P, 2.3 µM; SiO_2-Si, 50 µM. The amount of sediment was based on an assumption that subsurface sediment (down to 3 cm) could be evenly dispersed to a water column of 15 m depth, and the nutrient additions were in the past observed at the highest levels at the site. Two cultures were prepared and set under two different light levels; one under 250 µmol-photons m^{-2} sec^{-1} determined by a calculation of the light level at 3 m depth on a sunny day in June, and another under 50 µmol-photons m^{-2} sec^{-1} on a cloudy day in June (14:10 h light: dark cycles). The simulation at the 3 m depth was based on our experience at the site where riverine water from Ohta River largely affected the subsurface layer (0–2 m), and thus at the 3 m depth, it has less effect on riverine water, but has sufficient light level. The incubation was performed at 21°C, which is a temperature similar to the scheduled plowing season in June.

2.3 An overview of sea-bottom plowing

Figure 1C shows the plowing areas; Area C1 covering 0.8 km^2 was for 2018, area C2 (0.9 km^2) was for both 2019 and 2021, and area C3 (0.3 km^2) was for 2020. Sea-bottom plowing was conducted for continuous three days of June 4th–6th in 2018, June 10th–12th in 2019, and 15th–17th in 2020 and 2021. June is the beginning of the oyster spawning season when enough phytoplankton supply is expected. On each date, plowing was performed for 2–5 hours in the morning using special-made plowing gears (Figures 2A, B) which were dragged by fishermen's boats (Figure 2B). A total of nine or 10 boats were engaged in the plowing activity each day.

2.4 Field monitoring and analyses of water samples

Field monitoring was conducted right before, right after, and two days later (2018 and 2019) or five days later (2021) after the plowing activities. The average residence time of water masses in the northern part of Hiroshima Bay is 2-3 days (Kawanishi, 1999), and it is considered that the effect of plowing after 5 days might be small for the data. At the center of the plowing area (black circles in area C1, C2, or C3 in Figure 1C), vertical profiles of water temperature, salinity, chl. *a* fluorescence, and downward PPFD were measured by Hydrolab DS5 CTD (OTT HydroMet, Colorado, USA). Turbidity was measured by ASTD 675 CTD (JFE Advantech, Hyogo, Japan). Water samples were taken from depths of 1, 3, 5, 10, and the bottom-1 m using a Van Dorn water sampler (note that samplings at a surface layer were added in 2020 and 2021). Similar CTD measurements and water collections were also made at the control areas for referencing the plowing effect at the points in area C1 in 2019, area C3 in 2021, and C4 in 2020 (black circles in Figure 1C). The activity in 2018 missed the control area. In the control area of 2020, water samples were collected only from 0, 3, and bottom-1 m depths, and these samples were used only for nutrient analysis (details described below).

Sigma-*t* was calculated from the water temperature and salinity measurements by CTD, and a temperature/salinity (TS) diagram was made using Ocean Data View software (Schlitzer, 2018). The collected water samples were filtered through a 0.45-µm syringe filter and subjected to a measurement of dissolved inorganic nutrients (DIN: NO_3 + NO_2 + NH_4-N, PO_4-P, SiO_2-Si) using a nutrient autoanalyzer (SWAAT, BLTEC, Tokyo, Japan). One milliliter of each water sample was microscopically examined for phytoplankton occurrences. To access the risk of harmful phytoplankton, 500 mL of water samples collected at depths of 1, 3, 5, and 10 m were concentrated to 50-fold by gravity filtration using a membrane filter (5 µm pore-size). A total of 100 ml of the water samples were also filtered using glass microfiber filters and infiltrated with N,N-dimethylformamide to measure chl. *a* concentration using a fluorometer (10 AU, Turner Designs, California, USA) based on Holm-Hansen et al. (1965). The determined chl. *a* concentrations were used to calibrate CTD and determine the primary production rate.

2.5 Photosynthetic parameters and primary production

To evaluate the effect of sea-bottom plowing on primary productivity, photosynthetic carbon fixation in the water columns was estimated using a pulse amplitude modulation (PAM) fluorometry based on protocols reported by Maung-Saw-Htoo-Thaw et al. (2017) and Ohara et al. (2020). Conceptually, electron transport rates (ETR) from the photosystem II in a plant (in our case, phytoplankton) under various light intensities were determined for the water samples obtained from 1, 3, 5, 10, and bottom-1 m depths by a cuvette-type PAM fluorometer (Water-PAM, Heinz Walz, Effeltrich, Germany). By inputting desirable light intensity to this model-fitted ETR vs light curve, unit area- and unit time-based ETR (µmol electron m^{-2} s^{-1}) was determined. This value was then multiplied with the so-called chlorophyll *a*-specific absorption cross section (m^2 mg-chl. a^{-1}) to obtain another value

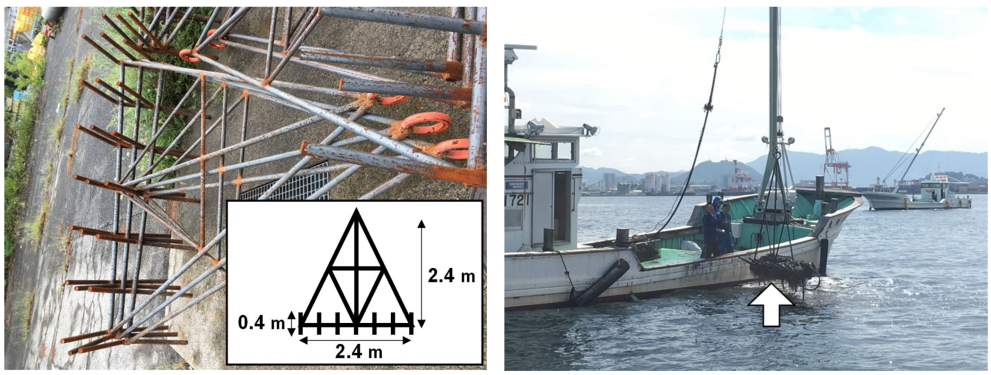

FIGURE 2
A photograph and a schematic drawing (an insertion) of the plowing gear **(A)**, a fisherman's boat used for the plowing **(B)**. The boat in the photograph is hanging the plowing gear to collect garbage (B, arrow).

normalized to chlorophyll *a* concentration in the tested seawater (μmol electron mg-chl.a^{-1} s^{-1}). This value was then converted to oxygen evolution by an assumption of 4 mol e^- = 1 mol O_2 (Gilbert et al., 2000) and further to carbon weight using a carbon assimilation factor (photosynthesis quotient, 1.3) (Platt et al., 1987). The chlorophyll *a*-normalized carbon assimilation rates determined for every 0.5 m depth interval, and by multiplying with chl. *a* concentration in the water volume (i.e., 1 x 1 x 0.5 m), were integrated from the sea surface (0 m) to the bottom, and a primary production rate of the water column (1 x 1 x bottom depth) was obtained. Such calculation can be made for any desirable depth zone by adjusting integrating depth. In this study, the model-fitted ETR vs light curves were calculated at 1, 3, 5, 10, and 12 m depths; the curve of 1 m was used for the 0–2 m zone, that of 3 m was for the 2.5–4 m, that of 5 m was for the 4.5–7.5 m, that of 10 m was for the 8–11 m, and that of bottom-1 m was for the 11.5 m–bottom. Other than the above ETR-based primary production, a maximum photosynthetic yield under dark conditions (*Fv/Fm*) was also determined. In 2018 and 2020, *Fv/Fm* and primary production rates were measured only in the plowing area but not in the control area.

2.6 Culture experiment

Although the culture experiment carried out as a preliminary survey in 2018 was carried out under sufficient nutrient conditions, the nutrient concentration in the sampling area was lower. Therefore, we conducted the following culture experiments in 2021 without adding inorganic nutrients. In 2021, sediment samples and seawater from a 3m depth were collected from the scheduled plowing area (area C2) right before the plowing activity and used to simulate the plowing effect in a laboratory. Three experimental batches were prepared: 1) The one g sediment was added to the 5 L seawater in a PET bottle, based on the assumption described in 2.2, to know the total phytoplankton growth (both originating from the sediment and seawater). 2) This is similar to (1) but the sediment was added to the seawater filtered by a glass fiber filter (GF/F) to know if the phytoplankton growth originated from the sediment only. 3) Non-filtered seawater without sediment addition to determine the phytoplankton growth originally in the seawater. Each bath was done in a triplicate manner thus giving a total of nine bottles. They were placed in an incubator where the temperature and light were set to 21°C and 250 μmol-photons m^{-2} sec^{-1}. Phytoplankton taxa and abundances were monitored for 9 days.

2.7 Statistical analyses

Significant differences ($p < 0.05$) between the daily means of the revised chl. *a* concentration at depths of 2.5–7 m for 2018, 2020, and 2021 and 5–7 m for 2019 in the plowing and control areas were examined with a Tukey-Kramer test followed by one-way analysis of variance (ANOVA) using R version 3.5.1 (R Core Team, 2018).

3 Results

3.1 Abundance of the resting stage cells

The estimated densities of diatoms ranged within 1.5–2.6×10^5 MPN g^{-1} wet sediment (Figure 3A) and predominantly consisted of a genus *Skeletonema*, which accounted for 61.6 – 89.1% of all diatoms. *Chaetoceros* was the second dominant genus accounting for 6.5 – 20.8%. Both genera plus the third dominant genus of *Thalassiosira* were 80.2–95.6% of the total populations of the diatoms' resting stage cells. Due to the nature of the sediment, pennate diatoms were also found but accounted for only 1.9-19.8% of the total population. The total densities of flagellates' cysts, mostly of dinoflagellates and raphidophytes, were 0.2–0.6×10^3 MPN g^{-1} wet sediment (Figure 3B), which were almost 1/1000 of the diatoms' occurrences. Among them, a raphidophyte *Heterosigma akashiwo* is recognized as a potentially harmful species that may cause fish-kill, but it occurred only in 2018 and was 1.5×10^2 MPN g^{-1}; the value was almost 1/1000 of the diatoms recorded in 2018. Another concern had been an occurrence of toxic dinoflagellates that may cause shellfish poisoning, but they were not found.

3.2 Simulating germination potentials of phytoplankton species prior to the actual plowing

Prior to the first plowing activity in 2018, culture experiments were performed to know the potential of germination in phytoplankton species, which could be possible by partly simulating phytoplankton increase after sea-bottom plowing (Figure 4). After 24 h of the sediment additions, diatoms' growth was recognized in both cultures under different light levels. While *Leptocylindrus danicus* was not initially recognized in the previous MPN experiments, they occurred after the 3rd day. Other diatom species, i.e., *Navicula* spp., *Chaetoceros* spp., and *Skeletonema* spp., were also found in the MPN experiments to have predominantly occurred by the 7th day. The cell numbers on the 5th and 7th days under the high-light condition were greater than those under the low-light condition, insisting that diatoms' occurrences by actual plowing might be reduced under cloudy or rainy weather conditions. As a raphidophyte, *Heterosigma akashiwo* was found in a relatively higher density in the sediment of 2018; it also occurred in the culture experiments but the density was as low as 1 cell mL^{-1}.

3.3 Actual plowing activities

3.3.1 Physicochemical parameters

Figure 5 shows a turbid sea surface during the plowing activity in 2019. Due to coastal currents, the plowing effect did not always appear right above the plowing area. Therefore, the below observations at the plowing area and the control area may not

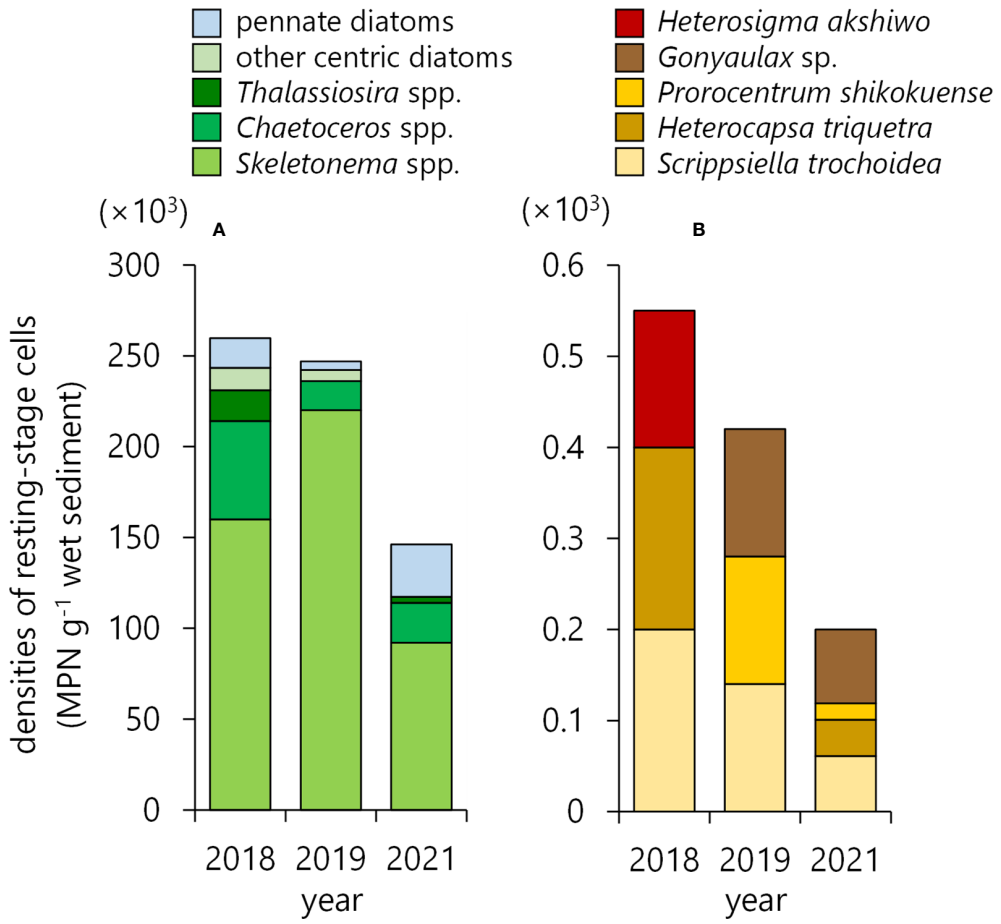

FIGURE 3
Densities of resting stage cells of diatoms **(A)** and cysts of non-diatom phytoplankton **(B)** in the sediments enumerated by a methodology of the most probable number (MPN). The sediments were collected at the plowing area (gray boxes in areas C1 and C2, Figure 1C) in 2018, 2019, and 2021.

exactly depict the effect of the plowing especially at the shallower depth. The subsurface zone (ca 1-2 m) was also largely affected by the river water. Figure 6 shows depth profiles of the CTD parameters, inorganic nutrients, and chlorophyll parameters. The water temperature, salinity, and resulting sigma-*t* explained a notable influence of the river water at the subsurface zone. TS diagrams (Figure 7) also show large fluctuations of subsurface water within the plowing period due to the river water. However, mid-deeper waters below 2.2 m (2018 and 2021), 4.7 m (2019), and 3.2 m (2020) were relatively homogenous and without large fluctuations of subsurface water. Therefore, zones deeper than those depths were considered to be influenced by the plowing activity. These zones were further separated by two layers, the middle layer and the bottom layer, based on light availability. We assumed that the minimum light level enabling the germination of diatom resting stage cells was 10 μmol-photons m^{-2} sec^{-1} (Itakura, 2000) and we determined that the depth available for this light level was 7.5 m (2018 and 2019), 12.0 m (2020), and 10.0 m (2021) based on the hourly global solar radiation from sunrise to sunset in June at the area (Japan Meteorological Agency, 2021) and the diffuse attenuation coefficient for the water column obtained from the CTD light sensor. The middle layer which was thus free from the subsurface fluctuation but shallower than these depths is shown in Figure 6.

Depth profiles of the dissolved inorganic nutrients (DIN: NO_3 + NO_2 + NH_4-N, PO_4-P, SiO_2-Si) are shown in Figure 6, and those averages at the bottom layer where the notable effect of the plowing was expected are summarized in Table 1. Another Table (Table 2) shows increased rates (x times) of these averages before and after the plowing. Although there are several exceptions where data is lacking in the control area (2018) or decreased PO_4-P in the plowing area (2020), data in the plowing area all showed ca. 1.2 – 4 times increase in the nutrients after the plowing activities.

Through the 4 years, the turbidity at the bottom layer increased drastically immediately after the plowing while that of the control areas was not obvious (Figure 6). The above-mentioned nutrient increase at the bottom layer seemingly coincided with the turbidity increase by the plowing activity. The middle layer was almost free from such turbidity or nutrient increase. One exception was in 2020 when there was notable precipitation leading to a drastic decrease in salinity and an increase in the nutrients at the surface layer, which might have caused nutrient increase even at the middle layer.

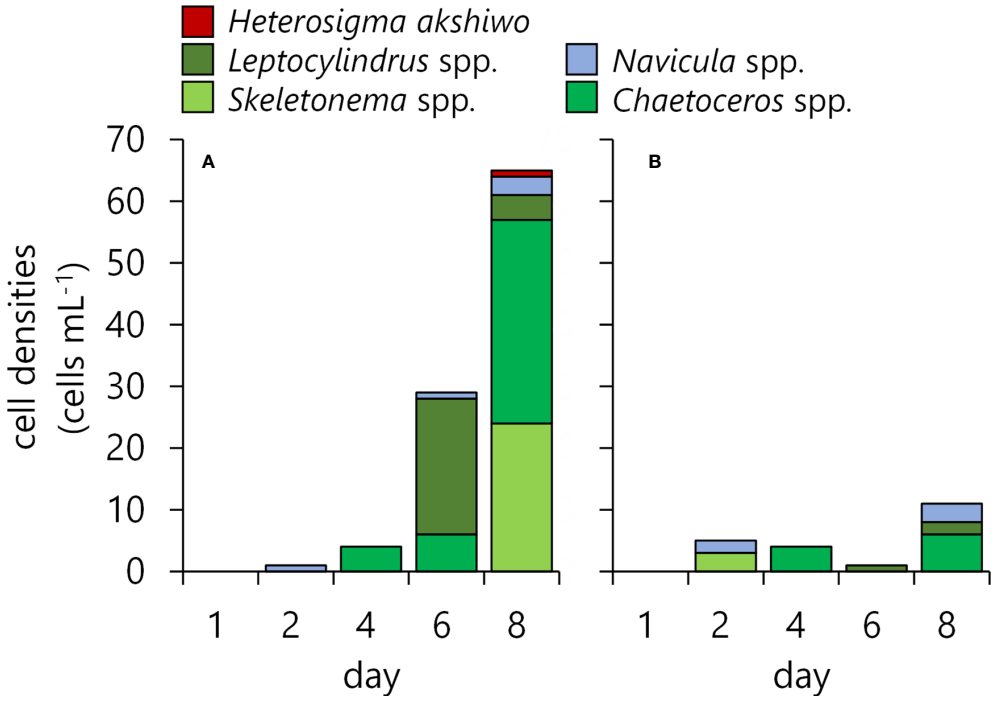

FIGURE 4
Germination and growth of the phytoplankton seeds in the sediment obtained in 2018. The left graph shows the result under high-light conditions (250 µmol photons m^{-2} sec^{-1}, **A**), and the right is under low-light conditions (50 µmol photons m^{-2} sec^{-1}, **B**).

3.2.2 Chlorophyll *a* concentration

As assumed above, the light level at the bottom layer was too low to promote diatoms' germination, and the surface layer was extensively affected by the river water. So, the middle layer is considered for observing possible diatoms' growth due to the plowing. Chlorophyll *a* data of the middle layer in Figure 6 were extracted and summarized as box plots in Figure 8. In 2018, while there was no statistical difference between the plowing area and the control area, chl. *a* concentrations after the plowing and 2 days later kept increasing from those prior to the plowing. More drastic and significant increases in the plowing area were observed in 2019. It surged to 1.89 times before and after the plowing. Similar but lesser increases of chl. *a* were also found in 2020. In 2021, chl. *a* concentration in the plowing area showed no significant change, but it became significantly larger in value by 1.69 times after 5 days from the initial value.

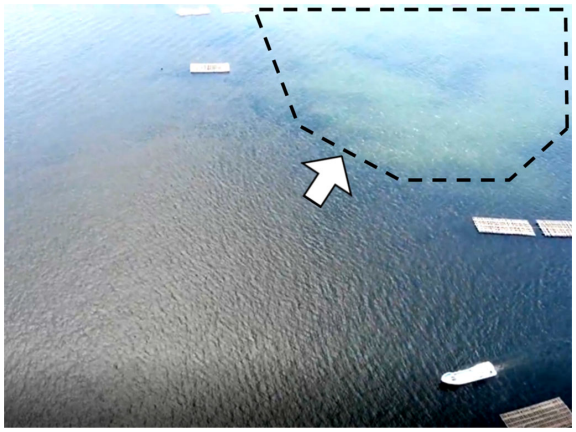

FIGURE 5
A photograph of the sea surface obtained by a drone during sea-bottom plowing in 2019. The sea surface became turbid due to sea-bottom plowing. The white arrow indicates the turbid area.

3.2.3 Photosynthetic parameters and primary production

Similar to the case of chl. *a*, primary production rates of the water column were estimated for the middle layer. Figure 9 shows transients of the ETR-based primary production rate (PPR_{ETR}) with diffuse attenuation coefficients (*k*, indices of turbidity) which largely affect the PPR_{ETR} estimation.

In 2018, while the control data was missing, PPR_{ETR} at the plowing area slightly dropped once after the plowing activity regardless of the increase in chl. *a* (Figure 8A) and/or increased photosynthetic activity (*Fv/Fm*, Figure 6A) but mostly due to increasing turbidity from k=0.272 to 0.435. After then, PPR_{ETR} at the plowing area suddenly increased almost two times higher than that before the plowing (Figure 9A), which was derived mostly from decreased *k* as well as maintained higher chl. *a* and *Fv/Fm* after the plowing.

In 2019, initial *Fv/Fm* values before the plowing maintained relatively higher values, and those changes were not obvious even after the plowing activity. Therefore, PPR_{ETR} was more affected by changes in chl. *a* and *k*. In the control area, as shown by the constant chl. *a* (Figure 8B) and by the constant *k* (Figure 9B), PPR_{ETR} also maintained relatively constant values. Meanwhile, that of the plowing area dropped once right after the plowing and surged

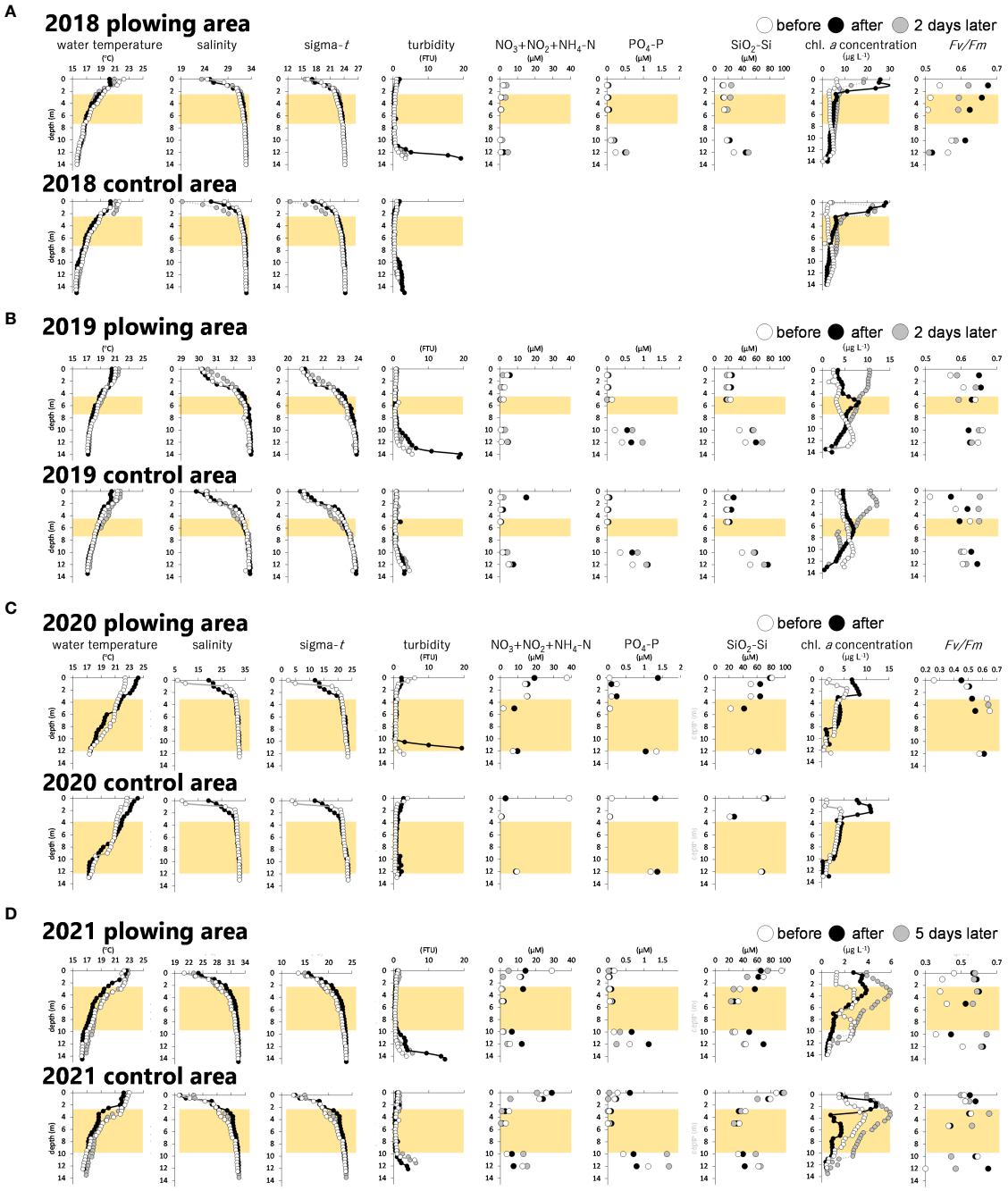

FIGURE 6
Vertical profiles of water temperature, salinity, density (sigma-*t*), turbidity, DIN (NO_3+NO_2+NH_4-N), PO_4-P, SiO_2-Si, and chlorophyll *a* (chl. *a*) concentration and maximum quantum yield of photosystem II (*Fv/Fm*) from the sea surface to the bottom in the plowing area and control area in 2018 **(A)**, 2019 **(B)**, 2020 **(C)**, and 2021 **(D)**. The middle layers which were free from the subsurface fluctuation but provided enough light for diatom germination (shallower than 7 m depth) were marked as yellow zones.

drastically 2 days later, similar to the case of 2018 which was mostly controlled by *k* (Figure 9B).

In 2020, although there was a slight increase in chl. *a* (Figure 8C) and a decrease in *Fv/Fm* (Figure 6C) in the middle layer, a drastic increase as well as an abnormally higher value of the PPR_{ETR} after the plowing was observed (Figure 9C). The *k* before plowing was abnormally high (k=0.509); it might be caused by high precipitation before the plowing. So, this increase in PPR_{ETR} was caused by the decrease in *k* (Figure 9C), and it is not an effect of the plowing.

In 2021, PPR_{ETR} either in the plowing area or the control area increased after the activity. Dissimilarly, from the previous years, there was no turbidity increase (i.e., *k*) in the middle layer at the plowing area that may have hindered PPR_{ETR} increase, and a more obvious decrease was recognized in the control area. This less turbid water at the control area led to an increase in PPR_{ETR}, but at the

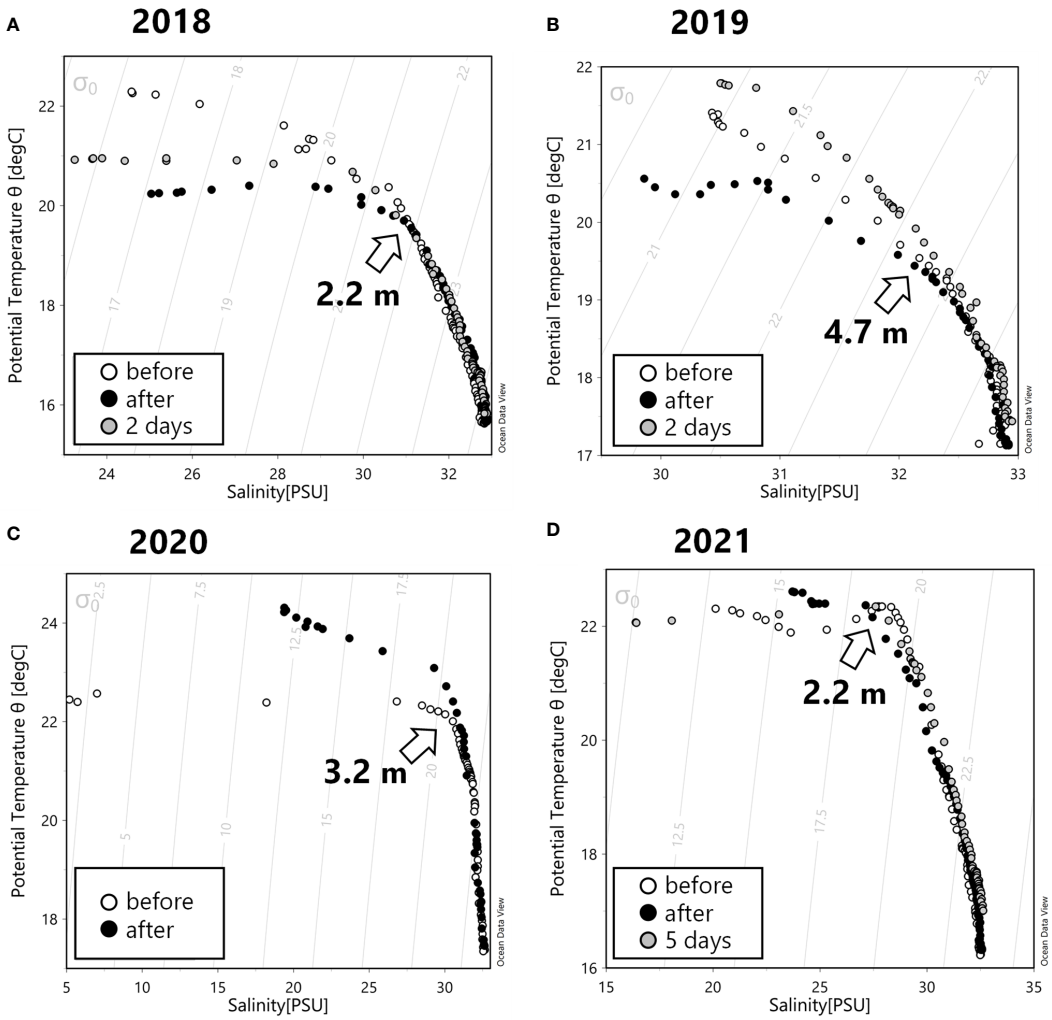

FIGURE 7
Temperature/Salinity (T/S) diagram in the plowing area in 2018 **(A)**, 2019 **(B)**, 2020 **(C)**, and 2021 **(D)** before (white circles), immediately after (black circles), and 2 or 5 days after (gray circles) sea-bottom plowings. The arrows indicate depths delineating the shallower zone that was largely affected by subsurface fluctuation and the deeper zone influenced by the plowing activity.

plowing area, increases in chl. *a* and *Fv/Fm* (Figure 6D) rather induced higher PPR_{ETR}. The PPR_{ETR} was still high after 5 days although it is not clear whether the plowing effect may prolong for such an extensive period.

3.2.4 Phytoplankton occurrence

Figures 10A, B show transients of phytoplankton occurrence, each categorized by phytoplankton taxa (I), major diatom genera and others (II), and flagellates (i.e., dinoflagellates, raphidophytes, and silicoflagellates) (III).

TABLE 1 Mean values of dissolved inorganic nutrients (DIN: NO_3+NO_2+NH_4-N, PO_4-P, and SiO_2-Si) at the bottom layer (averages of the values obtained from 10 m and bottom-1 m depths) in plowing areas and control areas before and after the plowing activity. The data for 2020 were from the bottom-1 m only.

(μM)	plowing area						control area					
	DIN		PO_4-P		SiO_2-Si		DIN		PO_4-P		SiO_2-Si	
year	before	after	before	after	before	after	before	after	before	after	before	after
2018	0.44	1.47	0.17	0.35	23.01	33.58						
2019	0.83	3.28	0.31	0.61	40.20	57.16	3.33	5.52	0.53	0.90	45.55	67.71
2020	7.11	9.62	1.33	1.04	51.58	61.99	9.27	8.78	1.18	1.36	66.06	67.73
2021	3.50	9.28	0.39	0.8	36.11	59.10	8.07	6.97	0.77	0.75	47.56	41.19

TABLE 2 Rates of increase in the dissolved inorganic nutrients (DIN: NO_3+NO_2+NH_4-N, PO_4-P, and SiO_2-Si) in the bottom layer are shown in TABLE 1.

(times)	plowing area			control area		
year	DIN	PO_4-P	SiO_2-Si	DIN	PO_4-P	SiO_2-Si
2018	3.30	2.07	1.46			
2019	3.94	1.95	1.42	1.66	1.70	1.49
2020	1.35	0.78	1.20	0.95	1.16	1.03
2021	2.65	2.30	1.64	0.86	0.98	0.87

In 2018, phytoplankton cells at 1 m depth mainly consisting of a diatom *Skeletonema* spp. were as high as 9,079 cells mL^{-1} before plowing and decreased to less than one-third of this value (2,562 cells mL^{-1}) immediately after plowing (Figure 10A, I). This was contradictory to the chl. *a* data (Figure 6A) probably because chlorophyll senescent cells were microscopically counted which would not be detected as chl. *a* data. This assumption was supported by the data of *Fv/Fm* which increased right after plowing (Figure 6A). In contrast with the trend at 1 m, phytoplankton occurrences at 3 m depth increased from 1,103 to 2,542 cells mL^{-1} after plowing and consisted of genera *Chaetoceros*, *Leptocylindrus*, and *Pseudo-nitzschia* (Figure 10A, II). While it was not obvious in the graph, *Chaetoceros* spp. increased from 0 to 30 cells mL^{-1} at a depth of 5 m. Other than diatoms (Figure 10A, III), dinoflagellate species *Prorocentrum shikokuense* and *Pr. triestinum* also increased after plowing. In an aim to know the unwanted effect of the plowing, especially at the oyster culture area, toxic dinoflagellates which may cause shellfish poisoning even at several 10 cells L^{-1} were separately enumerated by concentrating the water sample (See the materials and methods for details). The maximum density of a PSP (paralytic shellfish poisoning) causative species *Alexandrium pacificum* before plowing was 100 cells L^{-1} and decreased to 20 cells L^{-1} after plowing. It disappeared 2 days after plowing.

Diatoms were also major phytoplankton taxa in 2019 (Figure 10A, I) and increased gradually after plowing in both the plowing and control areas. The genus *Pseudo-nitzschia* was dominant at depths of 1, 3, and 5 m, where notable increases in diatoms were found (Figure 10A, II). Other diatoms showing obvious increases were the genera *Skeletonema* and *Chaetoceros*, with the highest concentrations of 1,930 cells mL^{-1} and 1,241 cells mL^{-1}, respectively, at a 1 m depth immediately after plowing. These changes in the cell numbers of phytoplankton taxa and diatom genera in 2019 were slightly larger in the plowing area than in the control area, but the trend was the same (Figure 10A, I and II). Similar to 2018, slight increases in non-diatom taxa were observed in the plowing and control areas (Figure 10A, III) and consisted of dinoflagellates *Pr. shikokuense*, *Pr. triestinum*, *Heterocapsa triquetra*, and *Scrippsiella trochoidea*. In the concentrated water samples, while the species was not recognized as a toxic species, *A. affine* was detected at 80 cells L^{-1} before plowing, and the cell density increased to 160 cells L^{-1} after plowing.

As already described in the previous section, 2020 was exceptional because of significant precipitation that continued before the plowing and massive phytoplankton blooms in the surface layer due to the extensive nutrient loads (Figure 6C). This bloom was mainly caused by the genus *Pseudo-nitzschia* (Figure 10B, II). Although not obvious as such diatom bloom, the dinoflagellate *Pr. triestinum* also significantly increased (Figure 10B, III). *A. pacificum* occurring at a cell density of 10 cells L^{-1} before the plowing slightly increased to 20 cells L^{-1} at 1 m depth.

In 2021, diatoms increased from 30 – 101 to 1,041 – 1,331 cells mL^{-1} in the plowing area at 0, 1, and 3 m depths right after the plowing (Figure 10B, I). Such increasements were larger than those of the control area which reached 104 – 744 cells mL^{-1} after the plowing and mostly accounted for the increases in genera *Skeletonema* and *Pseudo-nitzschia* (Figure 10B, II). Notable diatom increases were recognized in both the plowing and control areas in the surface layer after 5 days (Figure 10B, I and II), contributing to chl. *a* increase in Figure 8D, but it has been 5 days since the last plowing, and the impact of the plowing was considered to be small. Differently from the previous years, preliminary dominated silicoflagellates (*Dictyocha fibula*, *D. speculum*, and *Vicicitus globosus*) increased after the plowing in both areas (Figure 10B, III). *A. pacificum* initially occurring at a density of 40 cells L^{-1} almost diminished after the plowing.

3.2.5 Culture experiment using sediment and seawater in the plowing area

In 2021, sediment samples and seawater from a 3m depth were collected from the scheduled plowing area (area C2) right before the plowing activity and were used to simulate the plowing effect in a laboratory. As described above, the initial seawater before the plowing contained silicoflagellates as a dominant taxon. Incubating this seawater (without filtration) alone induced mostly *Pseudo-nitzschia* spp. growth, reaching 458 cells mL^{-1} on the sixth day (Figures 11A, B, I), which was followed by other pennate diatoms, *Skeletonema* spp., other centric diatoms, and *Chaetoceros* spp. Initially, dominated silicoflagellates almost disappeared along with those diatoms' growth. The addition of the sediment to this seawater induced other pennate diatoms' growth rather than *Pseudo-nitzschia* spp., and these pennate diatoms mostly consisted of *Cylindrotheca closterium* (Figures 11A, 11B, II). These pennate diatoms' growths including *Pseudo-nitzschia* spp. and *C. closterium* were negligible in the incubation experiment with filtered seawater plus bottom sediment, indicating they were of seawater origin. In this experiment, rather notable growths of *Chaetoceros* spp. and *Skeletonema* spp. reaching 1,165 and 554 cells mL^{-1}, respectively, on the ninth day (Figures 11A, 11B, III) supported the fact that they were of sediment origin as previously confirmed in Figure 3.

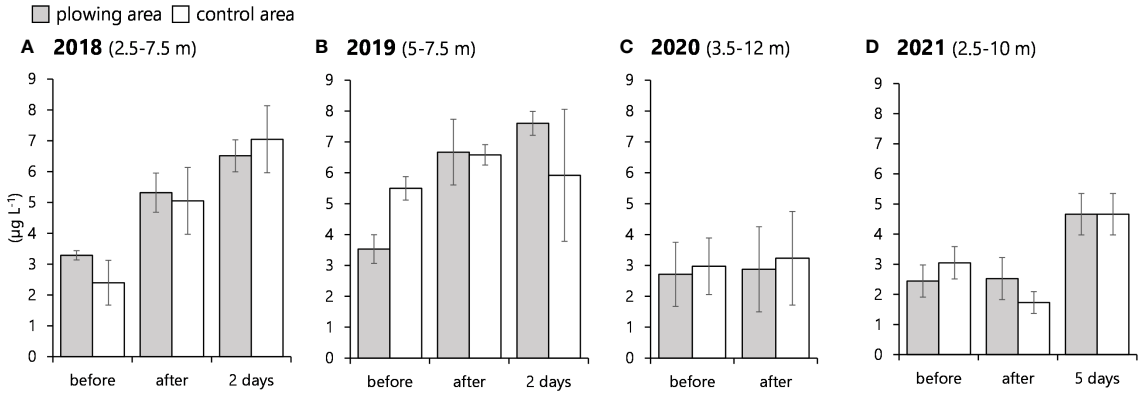

FIGURE 8
Box plots of chlorophyll *a* concentrations from a depth zone of 2.5–7 m for 2018 **(A)**, 2020 **(C)**, and 2021 **(D)**, and 5–7 m for 2019 **(B)** in the plowing and control area. The letters above each graph indicate a significant difference among the sampling dates ($p<0.05$, one-way ANOVA followed by the Tukey–Kramer test).

4 Discussion

4.1 Stimulation of diatoms' resting stage cells germination by sea-bottom plowing

To verify the effect of sea-bottom plowing on the increase in diatom levels, it was necessary first to confirm how many diatoms resting stage cells were present in the sediment and whether they were ready for germination in the natural environment. According to the preliminary surveys in 2018, 2019, and 2021, the bottom sediments contained 1.5–2.6×10^5 MPN g^{-1} wet sediment of germinable diatoms. This value was converted to 0.6–1.1×10^5 MPN cm^{-3} wet sediment (1 g wet sediment = 0.43 cm^3 wet sediment in 2021), and this was much more than the number of flagellates' cysts (0.9–2.6×10^2 MPN cm^{-3} wet sediment). Approximately 80% of the detected diatoms belonged to two genera, namely, *Skeletonema* and *Chaetoceros*. These results are similar to previous studies where the number of diatoms in the northern part of Hiroshima Bay was 1.3–3.6×10^5 MPN cm^{-3} wet sediment, consisting of only three species of the genera *Skeletonema*, *Chaetoceros*, and *Thalassiosira* (Imai et al., 1990; Itakura, 2000). Although the number of *H. akashiwo* cysts in this study ranged from below the detection limit to 0.6×10^2 MPN cm^{-3} wet sediment, a previous study using the same method as this study showed that the number of *H. akashiwo* cysts in the northern Hiroshima Bay was at most 5.6×10^1–2.9×10^4 MPN cm^{-3} wet sediment (Imai and Itakura, 1991). A culture experiment using the sediment collected in 2018 revealed that *Chaetoceros* spp. and *Skeletonema* spp. germinated from the sediment actually proliferated in water, and the germination and/or growth were largely affected by light intensity. At the time of actual plowing activities, the daily averages of the light at the middle layer calculated from the solar radiation and attenuation coefficient were 10.1 μmol-photons m^{-2} sec^{-1} (7.5 m) –88.8 (2.5 m) in 2018, 11.0 (7.5 m) –38.1 (5 m) in 2019, 10.8 (12.0 m) –162.3 (3.5 m) in 2020, and 10.9 (10.0 m) –122.5 (2.5 m) in 2021. When assuming that at least 10 μmol-photons m^{-2} sec^{-1} is required for diatom germination (Itakura, 2000), the middle layer could provide a not sufficient but minimal light environment for the dispersed diatoms' resting stage cells to germinate although their growth might be further controlled by the availability of higher light in the water column as shown in the culture experiment. It might be emphasized that *H. akashiwo* found in a

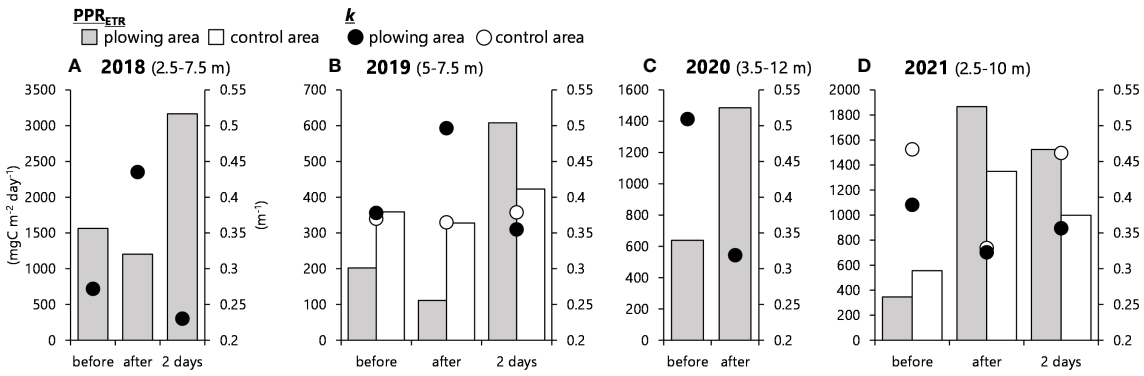

FIGURE 9
Diffuse attenuation coefficient (*k*, circles) and ETR (electron transport rate)-based primary production rates (bars) integrated from a depth of 2.5–7 m for 2018 **(A)**, 2020 **(C)**, and 2021 **(D)**, and 5–7 m for 2019 **(B)**. Filled circles and bars are the results of the plowing area, and open circles and bars are from the control.

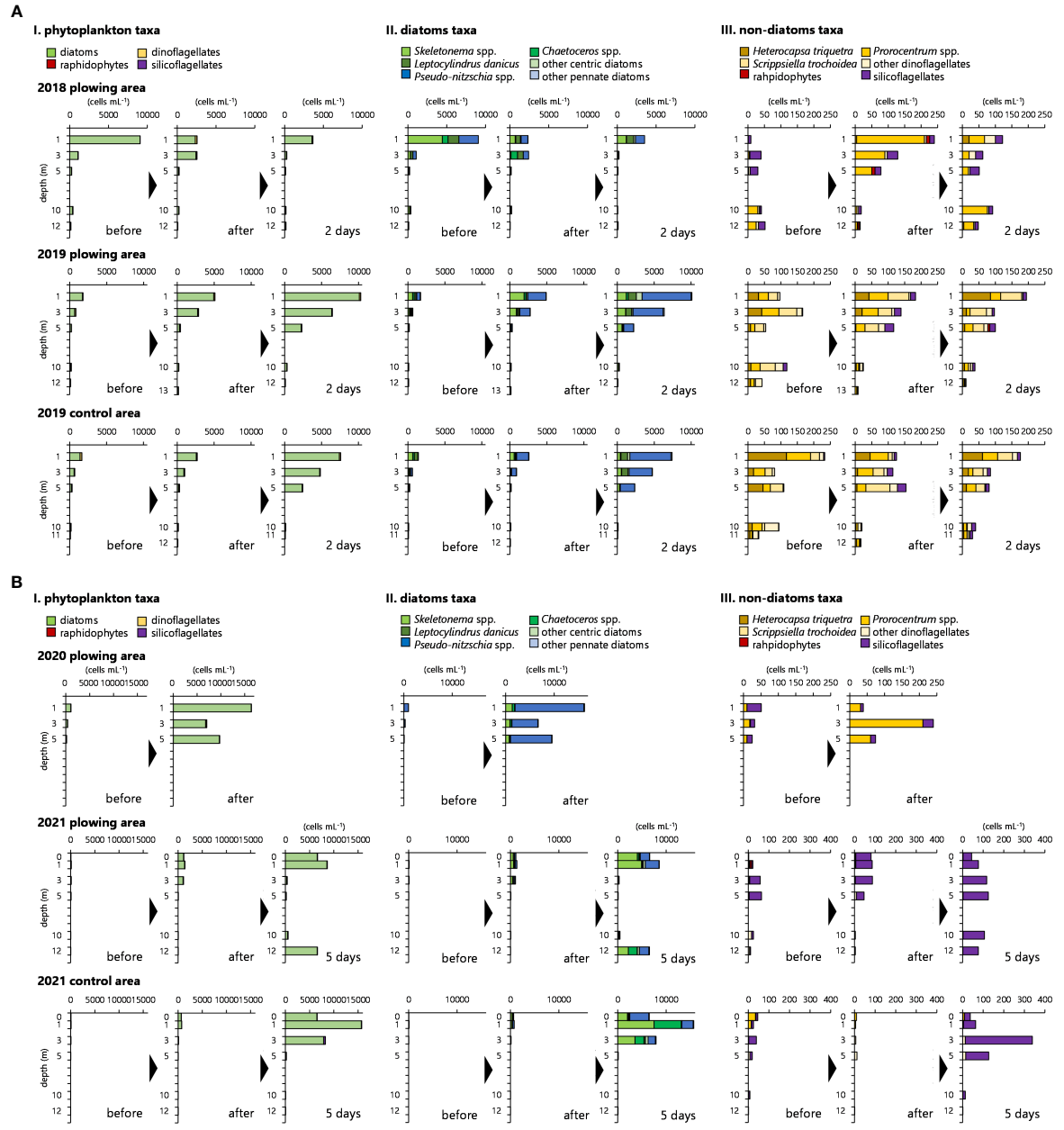

FIGURE 10
(A) Cell densities of each phytoplankton taxon (I), each diatom taxon (II), and each non-diatom taxon (III) at each sampling depth in the plowing area in 2018 and the plowing area and control area in 2019. **(B)** (continued from Figure 10A). Cell densities of each phytoplankton taxon (I), each diatom taxon (II), and each non-diatom taxon (III) at each sampling depth in the plowing area in 2020 and the plowing area and control area in 2021.

relatively higher density in the sediment of 2018 did not grow to overtake the diatoms (reached as low as 1 cell mL^{-1}), confirming less risk of unwanted flagellate blooming due to plowing activity.

4.2 Nutrient supply effect of sea-bottom plowing

The Seto Inland Sea, including Hiroshima Bay, has been reported to have undergone oligotrophy in recent years (Abo and Yamamoto, 2019), and the possible effect of plowing to supply nutrients is a matter of debate. Although there are several exceptions such as a lack of data in the control area (2018) or decreases in PO_4-P in the plowing area (2020), data in the plowing area all showed ca. 1.2 – 4 times increase in the nutrients at the bottom layer after plowing activities (Table 2). These nutrient increases seemingly coincided with the turbidity increases by the plowing activity and thus the nutrient stocks in the sediment were thought to be supplied. Similar effects due to plowing were found in Harima-Nada, Bisan-Seto, and Bingo-Nada all belonging to the Seto Inland Sea (Nakanishi et al., 2012; Imai et al., 2017; Ministry of the Environment, 2018). In anaerobic sediments, as is the case of Hiroshima Bay, the NH_4-N concentration in the sediment pore water is known to be high (Liu et al., 2003) because it is not nitrified

10.3389/fmars.2023.1222810

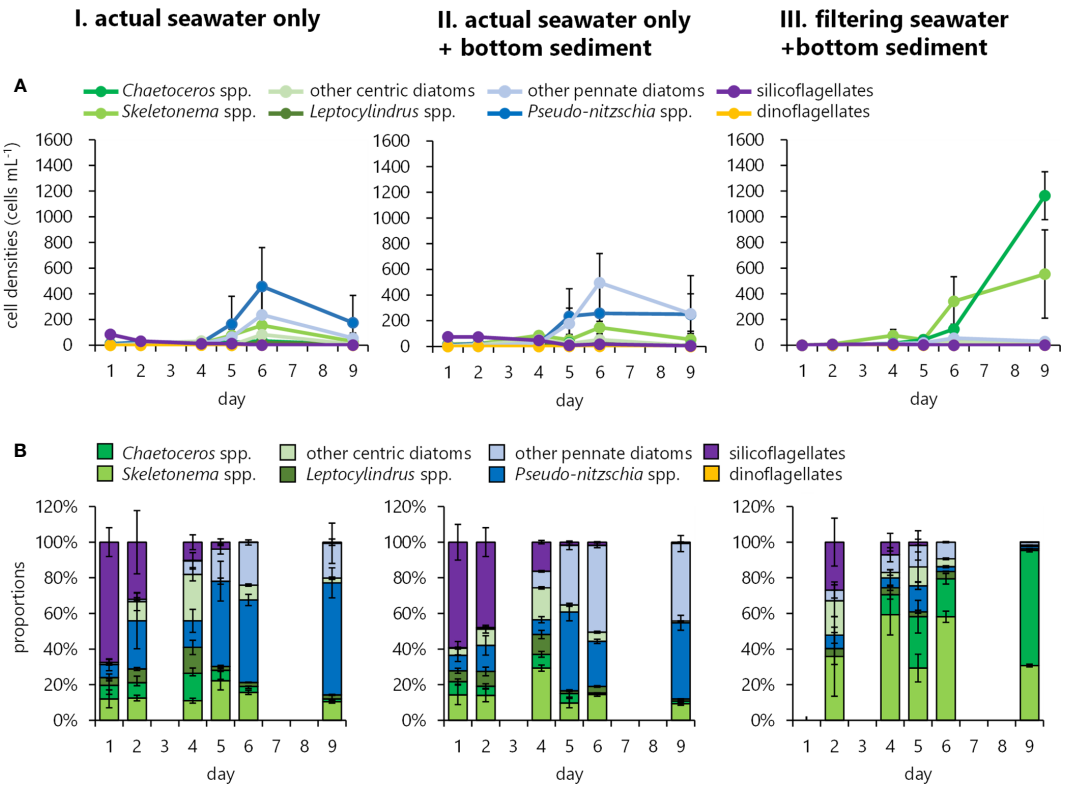

FIGURE 11
Simulation of phytoplankton occurrences and growth in an incubation experiment using sediment samples and seawater from 3m depth collected prior to the plowing activity in 2021. The cell densities **(A)** and proportions of occurring phytoplankton taxa **(B)** are shown for I) Non-filtered seawater without sediment addition, II) Non-filtered seawater with sediment (one g to 5L seawater), and III) Filtered seawater with sediment.

under anaerobic conditions. In addition, under aerobic conditions, PO_4-P is adsorbed by iron (II) oxide to form insoluble Fe (III)-PO_4 particles (Krom and Berner, 1980), but under anaerobic conditions, part of the iron (II) oxide is reduced, and PO_4-P is eluted (Middelburg and Levin, 2009; Thouvenot-Korppoo et al., 2012). Therefore, NH_4-N and PO_4-P abundantly existing in the interstitial and overlying water of the sediments were expected to be supplied to the above water column by plowing.

4.3 The influence of sea-bottom plowing on primary production and phytoplankton occurrence

With those nutrient supplies by plowing and based on the potential of the diatoms' germination from the sediments, primary production is expected to increase. ETR-based primary production rates (PPR_{ETR}) of the water column estimated for the middle layer (Figure 9) showed that both in 2018 and 2019, PPR_{ETR} at the plowing area decreased once after the plowing activity and suddenly increased more than before the plowing. The cases in 2020 and 2021 were free from such temporary drops and showed immediate increases after the plowings. The PPR_{ETR} was calculated by three parameters: light, chl. *a* concentration, and photosynthetic activity. Because the water became turbid due to plowing, as indicated by increases in diffuse attenuation coefficient (*k*, Figure 9), PPR_{ETR} once decreased after the plowing in 2018 and 2019, regardless of significant increases in chl. *a* in both years and regardless of a significant promotion of *Fv/Fm* in 2018. The relaxation of *k* after two days thus resulted in a significant increase in PPR_{ETR}. In 2020 and 2021, although chl. *a* did not increase significantly, the PPR_{ETR} increased. The *k* decreases in 2020 and 2021 also led to increased PPR_{ETR}, considering the fact that the bottom layers were turbid enough due to the plowing (Figures 6C, D). PPR_{ETR} calculation in estuaries in this study area could be largely affected by turbidity due to factors other than plowing, such as the inflow of turbidity from rivers, and therefore the effect of the plowing sometimes may not be relevant. As a next step, we focused on chl. *a* increase or increase in photosynthetic activity.

In 2018, chl. *a* (Figure 8A) and *Fv/Fm* (Figure 6A) increased in the middle layer after plowing, suggesting increased photosynthetic activity as indicated by increased *Fv/Fm*, leading to an increase in phytoplankton. Meanwhile, such chl. *a* increase did not always coincide with a cell density increase in phytoplankton. For example, *Skeletonema* spp. occurring as high as 9,079 cells mL^{-1} at 1 m depth before the plowing decreased to less than one-third (2,562 cells mL^{-1}) after the plowing (Figure 10A, II), while the chl. *a* value increased 4.37 times. Such contradiction could be partly explained by the fact that the initial population mostly consisted of less chloroplastalized cells which were then vitalized as shown by *Fv/Fm* increase that would further lead to increases of chl. *a* per cell capita. In the middle layer, a spot increase in *Chaetoceros* spp. at 3 m depth (Figure 10A,

II) was also along with *Fv/Fm* increase (Figure 6A) which might be attributed to the plowing effect. Rather, species other than diatoms and dinoflagellates *Prorocentrum* spp. (*Pr. Shikokuense* and *Pr. triestinum*) drastically increased at 1, 3, and 5 m depths (Figure 10A, III). Among them, *Pr. triestinum* is known to form a cyst (Bursa, 1959) and therefore might be supplied by the plowing activity although this was not primarily evidenced by the culture experiment in Section 3.2.

A more drastic increase in chl. *a* at the middle layer in the plowing area was observed in 2019 (Figure 8B). While *Fv/Fm* increased more at the surface layer (Figure 6B) probably due to riverine water, the values in the middle layer were seemingly high (> 0.6) even before the plowing and remained constant even after the activity. So, the effects of plowing to stimulate photosynthetic activity and chl. *a* increases were not clear in this case. Genera *Pseudo-nitzschia* and *Skeletonema* were the first and the second dominant diatoms in the middle layer and increased 2.78–12.35 times and 2.26–4.36 times, respectively, after the plowing (Figure 10A, II). *L. danicus* also increased at the 3 m depth. *Skeletonema* spp. and *L. danicus* are the species forming resting stage cells (e.g., French and Hargraves, 1986; Imai et al., 1990) and might be considered to be derived from the plowing. In contrast, the genus *Pseudo-nitzschia* is not known to form resting stage cells (Lelong et al., 2012) and is also not detected in the MPN enumeration (Section 3.1) and the germination experiments (Section 3.2). Therefore, the initial *Pseudo-nitzschia* community in the water column might increase after the plowing. In 2019, non-diatoms, especially dinoflagellates, *Pr. shikokuense*, *Pr. triestinum*, *Heterocapsa triquetra*, and *Scrippsiella trochoidea*, increased at the 1 and 5 m depths after the plowing (Figure 10A, III). Except for *Pr. shikokuense*, it is reported that they form cysts (Bursa, 1959; Wall et al., 1970; Olli, 2004), and hence, sea-bottom plowing might cause this population increase.

In 2020, while a drastic increase in chl. *a* at the surface layer was found after the plowing (Figure 6C), there were no significant changes at the middle layer (Figure 8C), and the phenomenon was also true for *Fv/Fm* (Figure 6C). As indicated by the extremely low salinity in the surface layer (Figure 6C), heavy precipitation that continued by the beginning of the plowing conveyed large amounts of riverine nutrients. This caused initially high *Fv/Fm* in the middle layer that could not be further promoted by the plowing. The drastic increase in chl *a* in the surface created an unneglectable effect even to the middle layer which further made the effect unclear. The increase in phytoplankton cells in the middle layer after the plowing (Figure 10B, I) should therefore not be interpreted as the plowing effect; in fact, the population increases were mostly due to *Pseudo-nitzschia* spp. that had been existing prior to the plowing (Figure 10B, II and III), and the contributions of sediment-derived genera, i.e., *Skeletonema* spp. and *Chaetoceros* spp. were quite low.

In 2021, while it was not significant, chl. *a* increase in the middle layer after the plowing was recognized, and it became even higher 5 days later (Figure 8D). Similarly in 2018, *Fv/Fm* largely increased after the plowing (Figure 6D), and this high photosynthetic activity might lead to chl. *a* increase. Diatoms *Skeletonema* spp. and *Pseudo-nitzschia* spp. increased 11.72 times and 28.11 times, respectively, after the plowing at 3 m depth (Figure 10B, II). In 2021, the culture experiment was conducted using the pre-plowing seawater of 3 m depth and the bottom sediment at the plowing area as described in Section 3.2.5. Incubating the seawater without filtration alone induced mostly *Pseudo-nitzschia* spp. growth (Figures 11A, B, I) and that of filtered seawater with sediment addition induced *Chaetoceros* spp. and *Skeletonema* spp. (Figures 11A, B, III), suggesting *Pseudo-nitzschia* spp. were of seawater origin and the other two genera were mostly of sediment origin.

As emphasized above, plowing may also induce dinoflagellates' germination and growth. One of the main concerns should be the unwanted growth of toxic species, especially in our study area of oyster culture. A dinoflagellate genus *Alexandrium*, which contains cyst-forming species (Anderson, 1998; Band-Schmidt et al., 2005) and the species causing PSP, were therefore carefully monitored using concentrated seawaters. In 2019, a non-toxic species, *A. affine*, increased after plowing, but existence at the maximum abundance of 80 cells L^{-1} in the seawater before the plowing suggested that the plowing activity did not necessarily provide seed population, but the initial population could increase in the water column. In 2018, 2020, and 2021, *A. pacificum*, a toxic species, was found before the plowing, but the abundance decreased in 2018 and 2021 or maintained a low level in 2020 after the plowing. Though yet unproven, a report of another plowing activity suggested that increased diatoms could suppress flagellates' growth (Imai et al., 2017).

4.4 Summary of the verified effects of sea-bottom plowing

This study examined whether enriching diatoms in the water column by sea-bottom plowing is possible through laboratory experiments and field surveys. Laboratory experiments revealed that diatom resting stage cells were abundant in the study area. In contrast, noxious flagellate resting stage cells were present in only approximately 1/1000 of diatoms. The genera *Skeletonema* and *Chaetoceros* germinated and proliferated during plowing, especially in fine weather. In a field study of actual sea-bottom plowing, the increase in the abundance of *Skeletonema* spp. and *Chaetoceros* spp. thought to be caused by the germination of resting-stage cells, was confirmed. On the other hand, *Pseudo-nitzschia* increases were always observed after the plowing, probably due to the promotion of the seawater-originated population. These phytoplankton's photosynthetic activities and growths may also be promoted by increases in inorganic nutrients supplied from the bottom layer. This study confirmed the possibility that sea-bottom plowing has a novel effect of improving marine biological productivity (i.e., fishing field fertilization).

Data availability statement

The original contributions presented in the study are included in the article/supplementary material. Further inquiries can be directed to the corresponding author.

Author contributions

SO, KF, and KK conceived the idea of the study. All authors contributed to field samplings. SO conducted culture experiments. All authors contributed to the interpretation of the results. SO and KK drafted the original manuscript. KK supervised the conduct of this study. All authors reviewed the manuscript draft and revised it critically on intellectual content. All authors contributed to the article and approved the submitted version.

Funding

This work was supported by JSPS KAKENHI Grant Number JP20K21336 for KK.

Acknowledgments

The authors are grateful to the members of the Hiroshima City Fisheries Cooperative for supporting us during the sampling. We thank Masami Umeki and Yusuke Ohira of the Aquatic Ecology Laboratory of Hiroshima University for their assistance with our samplings and experiments.

Conflict of interest

The authors declare that the research was conducted in the absence of any commercial or financial relationships that could be construed as a potential conflict of interest.

Publisher's note

References

Abo, K., and Yamamoto, T. (2019). Oligotrophication and its measures in the seto inland Sea, Japan. *Bull. Jap Fish Res. Edu Agen* 49, 21–26.

Anderson, D. M. (1998). "Physiology and bloom dynamics of toxic *Alexandrium* species, with emphasis on life cycle transitions," in *Physiology and ecology of harmful algal bloom, NATO ASI series*, vol. G41 . Eds. D. M. Anderson, A. Cembella and G. M. Hallegraeff (Berlin: Springer), 29–48.

Band-Schmidt, C. J., Lechuga-Devéze, C. H., Kulis, D. M., and Anderson, D. M. (2005). Culture studies of *Alexandrium affine* (Dinophyceae), a nontoxic cyst forming dinoflagellate from bahía concepción, gulf of California. *Botanica Marina* 46, 44–54. doi: 10.1515/BOT.2003.007

Bursa, A. (1959). The genus prorocentrum ehrenberg. morphodynamics, protoplasmatic structures and taxonomy. *Can. J. Bot.* 37, 1–31. doi: 10.1139/b59-001

Core Team, R. (2018) *R: a language and environment for statistical computing* (Vienna, Austria: R Foundation for Statistical Computing). Available at: https://www.R-project.org/ (Accessed June 2018).

French, F. W., and Hargraves, P. E. (1986). Population dynamics of the spore-forming diatoms *Leptocylindrus* danicus in Narragansett bay, Rhode island. *J. Phycol* 22, 411–420. doi: 10.1111/j.1529-8817.1986.tb02482.x

Garrison, D. L. (1984). "Planktonic diatoms," in *Marine plankton life cycle strategies*. Eds. K. A. Steidinger and L. M. Walker (Boca Raton, Florida: CRC Press), 1–17.

Gilbert, M., Domin, A., Becker, A., and Wilhelm, C. (2000). Estimation of primary productivity by chlorophyll *a in vivo* fluorescence in freshwater phytoplankton. *Photosynthetica* 38, 111–126. doi: 10.1023/A:1026708327185

Hargraves, P. E., and French, F. W. (1983). "Diatom resting spores," in *Survival strategies of the algae*. Ed. G. A. Fryxell (Cambridge: Cambridge Univ. Pless), 49–68.

Hiroshima City Fisheries Promotion Center (2021) *Gyomu houkokusyo [Business report.]*. Available at: http://www.haff.city.hiroshima.jp/suisansc/gyoumuhoukoku.html (Accessed 31 August 2021).

Hollibaugh, J. T., Seibert, D. L. R., and Thomas, W. H. (1981). Observation on the survival and germination of resting spores of three *Chaetoceros* (Bacillariophyceae) species. *J. Phycol* 17, 1–9. doi: 10.1111/j.1529-8817.1981.tb00812.x

Holm-Hansen, O., Lorenzen, C. J., Holmes, R. W., and Strickland, J. D. H. (1965). Fluorometric determination of chlorophyll. *ICES J. Mar. Sci.* 30, 3–15. doi: 10.1093/icesjms/30.1.3

Imai, I. (2012). High growth rates of the red tide flagellate *Chattonella marina* (Raphidophyceae) observed in culture. *Bull. Fisheries Sci. Hokkaido Univ.* 62, 71–74.

Imai, I., and Itakura, S. (1991). Densities of dormant cells of the red tide flagellate *Heterosigma akashiwo* (Raphidophyceae) in bottom sediments of northern Hiroshima bay, Japan. *Bull. Japanese Soc. Microbial Ecol.* 6, 1–7. doi: 10.1264/microbes1986.6.1

Imai, I., Itakura, S., and Itoh, K. (1990). Distribution of diatom resting cells in sediments of harima-Nada and northern Hiroshima bay, the seto inland Sea, Japan. *oceanographic Soc. Japan* 28, 75–84.

Imai, I., Kakumu, A., Ohara, S., Yuki, T., Koike, K., Hagiwara, E., et al. (2017). Feasibility studies on sediment perturbation as control strategies for *Chattonella* red tides. *Bull. Fisheries Sci. Hokkaido Univ.* 67, 57–66.

Itakura, S. (2000). Physiological ecology of the resting stage cells of coastal planktonic diatoms. *Boll Fish Envion Inland Sea* 2, 67–130.

Japan Meteorological Agency (2021) *Kako no data kensaku [Database of the past meteorological data]*. Available at: https://www.data.jma.go.jp/obd/stats/etrn/index.php (Accessed 31 August 2021).

Kawanishi, K. (1999). Flow structure and sea water exchange characteristics of the northern waters of Hiroshima bay. *Proc. Coast. Engineering JSCE* 46, 1041–1045. doi: 10.2208/proce1989.46.1041

Koizumi, Y., Nishikawa, S., Yakushiji, F., and Uchida, T. (1997). Germination of resting stage cells and growth of vegetative cells in diatoms caused by kyucho events. *Bull. Japanese Soc. Fisheries Oceanogr* 61, 275–287.

Krom, M. D., and Berner, R. A. (1980). Adsorption of phosphate in anoxic marine sediments. *Limnol Oceanogr* 25, 797–806. doi: 10.4319/lo.1980.25.5.0797

Kuttippurath, J., Sunanda, N., Martin, M. V., and Chakraborty, K. (2021). Tropical storms trigger phytoplankton blooms in the deserts of north Indian ocean. *NPJ Climate Atmospheric Sci.* 4, 1–12. doi: 10.1038/s41612-021-00166-x

Lelong, A., Hégaret, H., Soudant, P., and Bates, S. S. (2012). *Pseudo-nitzschia* (Bacillariophyceae) species, domoic acid and amnesic shellfish poisoning: revisiting previous paradigms. *Phycologia* 51, 168–216. doi: 10.2216/11-37.1

Liu, S. M., Zhang, J., and Jiang, W. S. (2003). Pore water regeneration in shallow coastal bohai Sea, China. *J. Oceanogr* 59, 377–385. doi: 10.1023/A:1025576212927

Maung-Saw-Htoo-Thaw, O. S., Matsuoka, K., Yurimoto, T., Higo, S., Khin-Ko-Lay,, Win-Kyaing,, et al. (2017). Seasonal dynamics influencing coastal primary production and phytoplankton communities along the southern Myanmar coast. *J. Oceanogr* 73, 345–364. doi: 10.1007/s10872-016-0408-7

Middelburg, J. J., and Levin, L. A. (2009). Coastal hypoxia and sediment biogeochemistry. *Biogeosciences* 6, 1273–1293. doi: 10.5194/bg-6-1273-2009

Ministry of Agriculture, Forestry and Fisheries (2021) *Kaimen gyogyo seisan toukei tyousa [Fishery production statistics.]*. Available at: https://www.maff.go.jp/j/tokei/kouhyou/kaimen_gyosei/ (Accessed 31 August 2021).

Ministry of the Environment (2018) *Eiyouenrui no kanri ni kakaru jyunnoutekina torikumi no kentou [Consideration of an adaptive approach about managements of nutrients]*. Available at: http://www.env.go.jp/press/105150.html (Accessed 31 November 2021).

Nakanishi, T., Takase, H., Nakatani, A., and Imai, I. (2012). Study on "Cultivation of sea bottom" to adjust seawater nutrient imbalance. *J. Japan Soc. Civil Engineers Ser. B3* 68, I_1115–I_1120.

Ohara, S., Yano, R., Hagiwara, E., Yoneyama, H., and Koike, K. (2020). Environmental and seasonal dynamics altering the primary productivity in bingo-Nada (Bingo sound) of the seto inland Sea, Japan. *Plankton Benthos Res.* 15, 78–96. doi: 10.3800/pbr.15.78

Olli, K. (2004). Temporary cyst formation of *Heterocapsa triquetra* (Dinophyceae) in natural populations. *Mar. Biol.* 145, 1–8. doi: 10.1007/s00227-004-1295-9

Platt, T., Harrison, W. G., Horne, E. P. W., and Irwin, B. (1987). Carbon fixation and oxygen evolution by phytoplankton in the Canadian high arctic. *Polar Biol.* 8, 103–113. doi: 10.1007/BF00297064

Schlitzer, R. (2018) *Ocean data view*. Available at: https://odv.awi.de (Accessed 27 June 2018).

Setonaikai Fisheries Coordination Office (2021a) *Setonaikai no akashio [Red tide in the seto inland Sea]*. Available at: http://www.jfa.maff.go.jp/setouti/akasio/index.html (Accessed 31 November 2021).

Setonaikai Fisheries Coordination Office (2021b) *Kannai no gyogyou yousyokugyou no gaiyou [Summary of fish catches and aquacultures in seto inland Sea]*. Available at: http://www.jfa.maff.go.jp/setouti/tokei/ (Accessed 31 November 2021).

Tada, K., Monaka, K., Morishita, M., and Hashimoto, T. (1998). Standing stocks and production rates of phytoplankton and abundance of bacteria in the seto inland Sea, Japan. *J. Oceanogr* 54, 285–295. doi: 10.1007/BF02742613

Thouvenot-Korppoo, M., Lukkari, K., Järvelä, J., Leivuori, M., Karvonen, T., and Stipa, T. (2012). Phosphorus release and sediment geochemistry in a low-salinity water bay of the gulf of Finland. *Boreal Environ. Res.* 17, 237–251.

Tsuchiya, K., Yoshiki, T., Nakajima, R., Miyaguchi, H., Kuwahara, V. S., Taguchi, S., et al. (2013). Typhoon-driven variations in primary production and phytoplankton assemblages in sagami bay, Japan: a case study of typhoon mawar (T0511). *Plankton Benthos Res.* 8, 74–87. doi: 10.3800/pbr.8.74

Wall, D., Guillard, R. R. L., Dale, B., Swift, E., and Watabe, N. (1970). Calcitic resting cysts in *Peridinium trochoideum* (Stein) lemmermann, an autotrophic marine dinoflagellate. *Phycologia* 9, 151–156. doi: 10.2216/i0031-8884-9-2-151.1

Zeeman, S. I. (1985). The effects of tropical storm Dennis on coastal phytoplankton. *Estuarine Coast. Shelf Sci.* 20, 403–418. doi: 10.1016/0272-7714(85)90085-X